New Method for Ocean Disposal of CO_2 by a Submerged Kenics-Type Static Mixer

Hideo Tajima, Akihiro Yamasaki, and Fumio Kiyono
National Institute of Advanced Industrial Science and Technology, Tsukuba 305-8569, Japan

Ho Teng
AVL Powertrain Engineering, Inc., Plymouth, MI 48170

DOI 10.1002/aic.10083
Published online in Wiley InterScience (www.interscience.wiley.com).

A new method for ocean disposal of anthropogenic CO_2 is proposed. In this method, liquefied CO_2 is transported through a pipeline to a Kenics-type static mixer, submerged at a depth between 500 and 1,000 m below the ocean surface and mixed with seawater in the mixer and then released into the ocean. Because the pressure and temperature for seawater at depths $>$ 500 m satisfy those for hydrate formation, CO_2 hydrate may form at the CO_2–seawater interface. Thus, the release from the mixer is a mixture of liquid CO_2, hydrate, and seawater. The apparent CO_2 concentration of the release can be determined by the CO_2–seawater mixing rate and distribution of the CO_2 drops (with or without a hydrate layer) produced in the mixer. This proposed disposal method was simulated experimentally. The laboratory-scale simulation revealed that sizes of the dispersed CO_2 drops and their distribution in the mixer were governed by the mixing rate and the Weber number on the basis of the continuous phase (seawater); larger Weber numbers led to smaller drop sizes and more uniform drop distribution. It was also observed that the drops with a hydrate layer were generally smaller than those without a hydrate layer under the same mixing rate and that a fairly uniform distribution for the dispersed CO_2 drops was always obtained if the continuous-phase flow was fully turbulent. Results of the laboratory simulation suggest that the environmental impact induced by the CO_2 released by a Kenics-type static mixer may be better predicted than from conventional injection methods. *AIChE J,* 50: 871–878, 2004
Keywords: static mixer, Weber number, seawater, ocean disposal, anthropogenic CO_2

Introduction

Several scenarios for disposal and long-term sequestration of the anthropogenic CO_2 in the ocean have been proposed as a countermeasure to global warming (Halmann and Steinberg, 1999; Haugan and Drange, 1992; Kojima and Harrison, 1998; Steinberg, 1984). In these scenarios, CO_2 is captured from the postcombustion gases and then is released into the ocean in the form of gaseous CO_2 (Haugan and Drange, 1992; Saito et al., 2000), liquefied CO_2 (Herzog et al., 1997; Ozaki, 1997), dry ice (Nakashiki et al., 1991), or CO_2 hydrate (Saji et al., 1992; Yamasaki et al., 2000). The appropriate release depth changes with the buoyancy of the release in seawater and, therefore, varies with the form of the CO_2. The disposed CO_2, no matter in what form, is believed to dissolve fully in seawater and thus is sequestered in the ocean for a long period of time. Various factors, such as the form of the CO_2 and the release depth, the rate and concentration at the release site, sizes and motion of

Correspondence concerning this article should be addressed to H. Tajima at hideo-tajima@aist.go.jp.

the disperse CO_2 particles (that is, bubbles, drops, or solid particles—dry ice and hydrate being solid), the rate of dilution of the dissolved CO_2, and so forth, affect the environmental impact induced by the disposal. Only the disposal scenario having the minimum environmental impact would possibly be accepted by the public.

Among the scenarios proposed to date, disposal of liquid CO_2 in the ocean at intermediate depths has been considered to be the most feasible method on the basis of the cost and the ocean environmental impact induced by the CO_2 disposal. In this scenario, liquefied CO_2 is discharged through a submerged pipeline into the ocean at a depth between 500 and 1000 m. Because of the interfacial instability of the CO_2–seawater system, the liquid CO_2 efflux in seawater breaks up into drops (Teng et al., 1997). Liquid CO_2 is less dense than seawater at intermediate depths; thus, the CO_2 drops resulting from the disposal tend to ascend to the ocean surface. Because the ambient seawater is highly unsaturated with CO_2, if the sizes of the CO_2 drops are not very large, they will dissolve fully in seawater before reaching the phase change depth where CO_2 drops would turn into CO_2 bubbles. The CO_2-rich seawater is denser than that of the ambient seawater and thus it induces a negatively buoyant plume in the seawater (Liro et al., 1992), which transports the dissolved CO_2 to deeper depths where the CO_2 concentration will be diluted.

Because the pressure and temperature for seawater at depths $>$ 500 m generally satisfy those for hydrate formation [that is, $T < 283$ K and $p > 44.5$ bar (Song and Kobayashi, 1987)], CO_2 hydrate (a clathrate crystal with a stoichiometric formula of $8CO_2 \cdot 46H_2O$) may form at the CO_2–seawater interface. Formation of a thin layer of hydrate at the CO_2–seawater interface has been observed both in the ocean (Brewer et al., 1999; Sakai et al., 1990) and in laboratory simulations (Aya et al., 1992, 1993; Fujioka et al., 1994). Laboratory simulations indicate that the dissolution rate for the CO_2 drops covered with a hydrate layer is much smaller than that without a hydrate layer (Aya et al., 1992; Ogasawara et al., 2000). Thus, the CO_2 drops covered with a hydrate layer require longer dissolution distances than the same-size CO_2 drops without a hydrate layer. If the hydrate layer is thick enough, then it may turn the positive buoyancy of the CO_2 drops into negative because the CO_2 hydrate is denser than seawater.

The initial drop sizes, their distribution in the release, and their traveling distances in seawater are key parameters to analysis of the environmental impact induced by the disposal. Because the traveling distances of the CO_2 drops with or without a hydrate layer released in the ocean are affected significantly by their initial sizes, a relatively uniform drop distribution would permit easy evaluation of the environmental impact and prediction of the fate of the CO_2 released into the ocean (Sato and Hama, 2001). The initial drop sizes and their distribution in the release may be controlled relatively easily at a low discharge velocity. In such cases, however, an intermittent blockage of the orifices by hydrate might be encountered because of the buildup of CO_2 concentration in the vicinity of the injection orifices after a certain operation time. Intermittent hydrate blockage of natural CO_2 effluents from the seafloor has been observed in the hydrothermal field in the Okinawa trough (Sakai et al., 1990). Although increase in the discharge velocity would make the CO_2-efflux breakup time become shorter than that for hydrate formation and, therefore, the possible hydrate blockage could be prevented (Teng et al., 1997), a high discharge velocity may lead to a poor control of drop sizes because it results in multiple various-size drops with a highly nonuniform drop distribution in the release. Also, drop interactions are more frequent in a nonuniform drop distribution and the interacting drops may coalesce into large drops, resulting in variations in drop sizes after the release. Because dissolution distances of the released CO_2 drops vary with their initial sizes, it would be more difficult to predict the averaged dissolution distance for a release of various size drops with a highly nonuniform distribution than for a release of fairly uniform drop sizes and distribution.

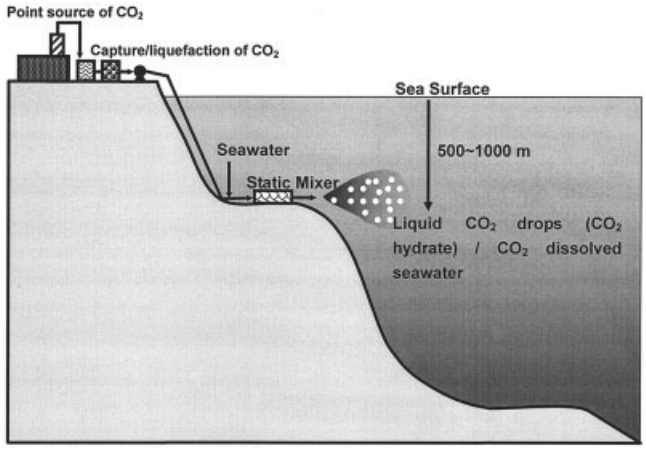

Figure 1. CO_2 ocean disposal scenario by a submerged static mixer.

To date, no study has been reported on preventing the possible intermittent hydrate blockage of discharge orifices and, at the same time, obtaining a manageable drop-size release. In this article, a solution to the aforementioned contradiction is proposed: disposal of liquid CO_2 by a submerged Kenics-type static mixer, which not only can prevent hydrate from blocking the discharge outlet but also can reasonably manage sizes of the CO_2 drops and their distribution in the release. Laboratory simulation of this new method will be reported in the following sections.

Release of Liquid CO_2 in the Ocean by a Kenics-Type Static Mixer: Concept

In the previously proposed scenario for ocean disposal of liquid CO_2 at intermediate depths, liquid CO_2 is discharged directly into the ocean through a submerged pipeline (Handa and Ohsumi, 1995). As was mentioned earlier, the direct disposal method may not simultaneously obtain a good control of drop sizes and prevent the orifice blockage by hydrate. To resolve this contradiction, a new method for releasing liquid CO_2 into the ocean is proposed here. The concept of this new method is described in Figure 1. In this concept, the captured and liquefied CO_2 is first transported into a release controller, a Kenics-type static mixer submerged in the ocean at a depth between 500 and 1000 m, where the liquid CO_2 is mixed with the low-temperature seawater. The well-mixed two-phase mixture, in which the liquid CO_2 is the dispersed phase and seawater is the continuous phase, is then released from the mixer into the ocean. The apparent CO_2 concentration of the

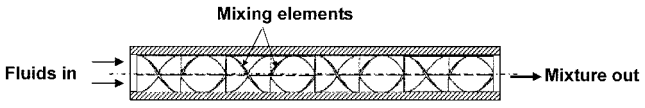

Figure 2. Structure of a Kenics-type static mixer.

release can be regulated by the mixing rate or the flow rate ratio of liquid CO_2 to seawater.

Figure 2 shows the structure of a Kenics-type static mixer used in the laboratory simulation for verifying the proposed concept. The cross-sectional area of the mixer is divided into two approximately semicircular passages by means of a number of helical thin partitions, the mixing elements or Kenics inserts. Each of the mixing elements is twisted through 180° and may be right- or lefthand rotation. Elements of alternate rotation are joined sequentially so that perpendicularity is maintained between the rearward and forward edges of adjacent elements. The liquid CO_2 and seawater flowing through the mixer are divided, rotated, and mixed by each of the mixing elements. If the mixing rate is properly controlled, then, after the mixture passes a certain number of the mixing elements, a disperse CO_2-drop flow can be obtained.

Releasing liquid CO_2 in the ocean by a static mixer has several features that may not be possible to the direct disposal method. First, the release is a CO_2–seawater mixture whose apparent CO_2 concentration can be regulated by the mixing rate; thus, the CO_2 concentration of the release can be adjusted according to the CO_2 concentration in the ambient seawater. Second, the static mixer serves as a drop producer. For a given mixer, the mean diameter of the CO_2 drops is governed primarily by the Weber number (which is a dimensionless parameter characterizing the stability of the dispersed phase); therefore, the mean drop diameter can be reasonably predicted for a given mixing rate and the corresponding Weber number (Berkman and Calabrese, 1988). This allows a good control of the postrelease mass-transfer process—drop dissolution in seawater. Third, because the pressure and temperature of the mixture satisfy those for hydrate formation, the mixer can also function as a hydrate crystallizer if the disposal in the hydrate form is preferred; in this case, sizes of the CO_2 drops must be small enough (close to the emulsion state) and their residence time in the mixer must be long enough to meet the requirement by the process of hydrate crystallization. This condition can be satisfied by simply adding more agitation elements, which is a common practice to make the dispersed phase emulsified in a Kenics-type static mixer. In the current study, the focus will be on the use of the first two features and consideration of the third feature is deferred.

Laboratory Simulation of the New Release Method: Experiment System

Figure 3 shows the experimental system for simulation of the proposed method. In the experiment, liquid CO_2 and water (respectively, from a CO_2 cylinder and a water tank) were pressurized then introduced into a Kenics-type static mixer. The purity of the liquid CO_2 was >99.9% (supplied by Showa Tansan Co., Ltd.) and the water was deionized and precooled to a desired temperature. The flow rate of the high-pressure CO_2 pump (product of Nippon Seimitsu Co., Ltd., NP-AX-70) could be adjusted in a range from 11.2 to 46.6 mL/min and the flow rate of the high-pressure water pump (product of Fuji Pump Co., Ltd., 2JN224-10V) could vary from 472 to 2063 mL/min. The static mixer was designed and made especially for the experiment (by Noritake Co., Ltd, based on their product of type 3/8-N10-522N). To simulate the pressure and temperature of seawater at intermediate depths, the mixer was designed to stand pressures up to 100 bar and with a cooling jacket (that is, it was of the mixer/heat exchanger type). The mixer was 210 mm long and 10.9 mm in inner diameter, and it had a total of 12 mixing elements with a length-to-diameter ratio of 1.5; the mixer was made of SUS316. A transparent polycarbonate section (10.6 mm in inner diameter and 300 mm in length) was in the downstream of the mixer for observing the release from the mixer. The temperature of the CO_2–water mixture was controlled by the cooling jacket, through which the coolant (a mixture of water and ethylene glycol) from a thermal bath was circulated. The temperature of the system could be controlled with an accuracy of ± 0.1 K. The pressure of the system was controlled by a pressure-regulating valve at the outlet of the flow system; at any set value, fluctuations in the system pressure were $< \pm 0.1$ bar.

The typical experimental pressure and temperature were, respectively, 7.0 MPa and 277 K, corresponding to those for seawater at a depth of 700 m below the ocean surface. The typical flows for liquid CO_2 and water were 23.2 and 472 mL/min, respectively, equivalent to an apparent CO_2 concentration of 4.38 wt % or a mixing rate of 21.84 kg water/kg CO_2. In the experiment, sizes of the CO_2 drops and their distribution in the release from the mixer could be observed in the observation section, and it was recorded by a 500-fps Photron video camera. The captured video data then were analyzed in a Power Macintosh G4 computer using the ImageJ-1.27 program developed by the U.S. National Institutes of Health.

Results and Discussion

Drop formation and size distribution in the static mixer

Because the CO_2–water system is inherently unstable, the liquid CO_2 introduced into water flowing in the static mixer disintegrated into CO_2 drops. This disintegration process took place in stages from liquid chunks/slugs from the initial breakup to disperse drops at the final stage. In the experiment, a disperse-drop flow could always be obtained by adjusting the

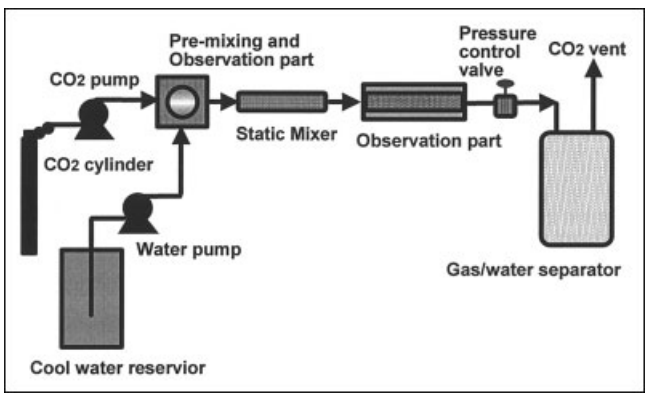

Figure 3. Experimental apparatus for simulation of the mixing behavior of liquid CO_2 and water flows in the static mixer.

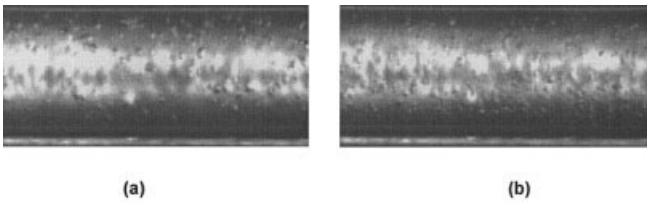

Figure 4. Typical disperse-drop flows observed after the static mixer.

Conditions: pressure = 7.0 MPa; temperature = 278 K; CO_2 flow rate = 46.6 mL/min; water flow rate = 1,573 mL/min (a) and 2,063 mL/min (b).

mixing rate or the ratio of the CO_2 to water flow. In a disperse-drop flow, liquid CO_2 became fully dispersed in water and, therefore, behavior of the CO_2 drops (the dispersed phase) was governed by the water (the continuous phase) flow. Figure 4 shows two typical cases of the disperse-drop flow in the static mixer.

Similarly to the situation in a direct-injection method, drops of various sizes were formed from breakup of the CO_2 flux in the mixer. However, many of these originally formed drops in the mixer were not stable and the dispersed drops in the release were those stabilized in the given flow condition. The stabilizing process of the CO_2 drops may be analyzed as follows. The stability of the CO_2 drops in the mixer is governed by their surface energy, which tends to stabilize the drops, and the disruptive energy associated with turbulent fluctuations in water, which tends to destabilize the drops. Because the drop breakup is attributed to the deformation induced by unstable surface waves formed on the drops, the disruptive energy is the energy that sustains the growth in amplitudes of the surface waves, which is provided by eddies whose linear scales are smaller than the drop diameters. For eddies whose linear scales are greater than the drop diameters and, therefore, greater than the maximum lengths of the surface waves on the drops, they transport the drops but barely induce the instability. When the drops become so small that their surface energy can subdue the growth of the surface waves, the drops are stabilized. The sizes of stable disperse drops vary with the intensity of turbulence in water and, therefore, vary with the water flow.

The average size of the disperse drops in the release is the basis for modeling the drop dissolution in seawater. The average size of the disperse drops may be described by the Sauter mean diameter (*SMD*), which is defined as

$$SMD = \sum N_i D_i^3 \Big/ \sum N_i D_i^2 \tag{1}$$

where N_i is the number of drops for the ith group having a diameter D_i. For the two disperse-drop flows given in Figure 4, the Sauter mean diameter, and ratios of the maximum drop size D_{max} and minimum drop size D_{min} to the Sauter mean diameter are, respectively, $SMD = 0.52$ mm, $D_{max}/SMD = 1.55$, and $D_{min}/SMD = 0.40$ for case (a); and $SMD = 0.38$ mm, $D_{max}/SMD = 1.61$, and $D_{min}/SMD = 0.53$ for case (b). Apparently, the drop sizes decrease and the drop uniformity increases with increase in the water flow.

The drop size distribution in the release provides the information on how well the drop dissolution is characterized by the mean drop diameter. The drop size distribution for the disperse-drop flow is found to obey a normal distribution with respect to the Sauter mean diameter; that is, the probability density for the drop size distribution can be characterized by

$$\frac{d(N/N_t)}{dD} = \frac{1}{\sqrt{2\pi}S_D}\exp\left[-\frac{(D - SMD)^2}{2S_D^2}\right] \tag{2}$$

where N is the number of drops with a diameter D, N_t is the total number of drops, and S_D is the standard deviation. The distribution function or the cumulative frequency then can be given in a form of the standard normal distribution as

$$N/N_t = \int_{-\infty}^{v} \frac{1}{\sqrt{2\pi}}\exp(-v^2/2)dv \tag{3}$$

where the integration is with respect to the dimensionless, relative drop size $v = (D - SMD)/S_D$. The corresponding probability density for the drop size distribution given by Eq. 3 is

$$P(D) = \frac{1}{\sqrt{2\pi}}\exp\left[-\left(\frac{D - SMD}{\sqrt{2}S_D}\right)^2\right] \tag{4}$$

Figures 5–7 show the statistical analysis results for the disperse-drop flows given in Figure 4: the sample for case (a) contained a total of 112 drops and the sample for case (b), 196 drops. It is seen in Figures 5–7 that the drop size distributions and mean drop diameters for the two disperse-drop flows are well characterized by the normal distribution and the Sauter mean diameter.

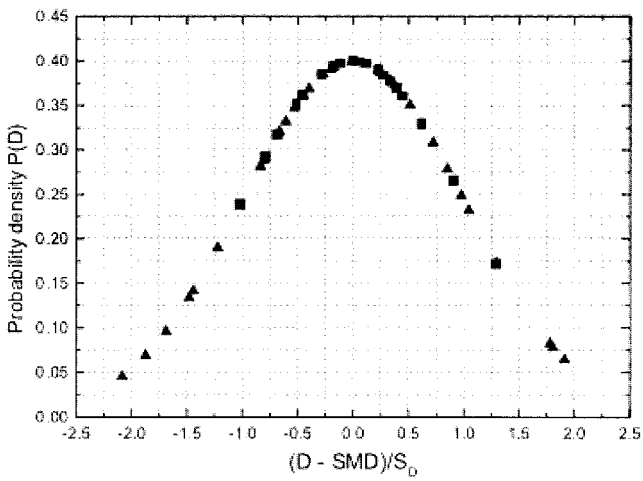

Figure 5. Size distributions of the liquid CO_2 drops in the disperse-drop flows for the conditions same as in Figure 4: ■, case (a); ●, case (b).

Conditions: pressure = 7.0 MPa; temperature = 278 K; CO_2 flow rate = 46.6 mL/min; water flow rate = 1,573 mL/min (a) and 2,063 mL/min (b).

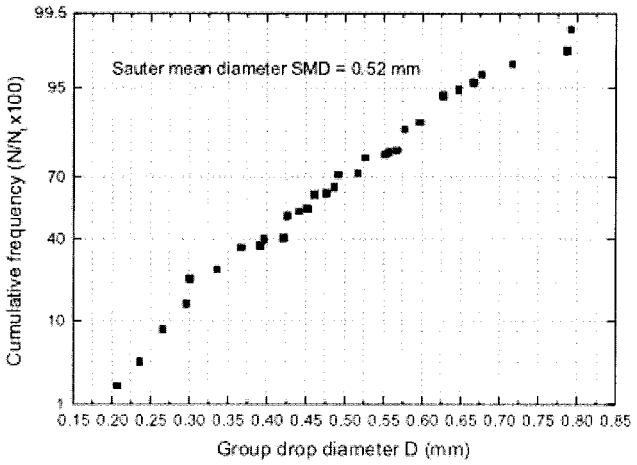

Figure 6. Cumulative frequency of the CO_2 drop diameter observed for case (a) in Figure 4.

Conditions: pressure = 7.0 MPa; temperature = 278 K; CO_2 flow rate = 46.6 mL/min; water flow rate = 1,573 mL/min.

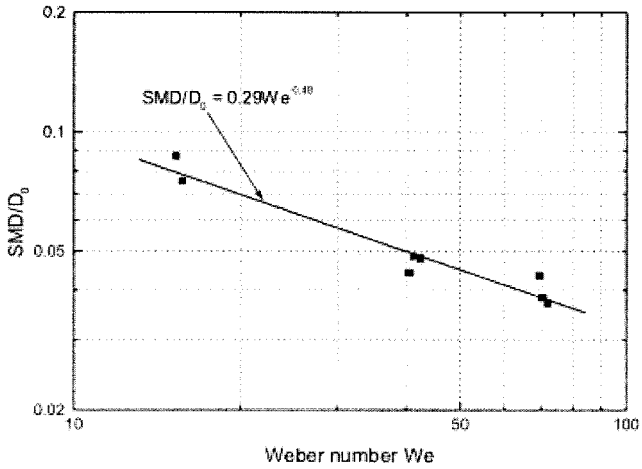

Figure 8. Dependency of the nondimensionalized Sauter mean diameter (SMD) on the Weber number (We) for the liquid CO_2 drops in disperse-drop flow observed after the static mixer.

Influence of continuous-phase flow on drop sizes

As is indicated by Eq. 1, *SMD* is a volume-to-surface mean diameter. Because the disruptive energy that a drop is subject to is proportional to the drop volume and the drop surface energy is proportional to the surface area of the drop, *SMD* may be expressed as a function of the ratio of the disruptive to the surface energy as

$$SMD/D_0 = f(E_d/E_s) \tag{5}$$

where D_0 is the inner diameter of the mixer, $E_d = (\pi/6)D^3\rho e_d$ is the magnitude of the disruptive energy, D is the drop diameter, ρ is the density of water, and e_d is the disruptive energy for unit-mass of water or specific disruptive energy; $E_s = \pi D^2\sigma$ is the drop surface energy and σ is the interfacial tension. Because the disruptive energy is dissipative, the magnitude for e_d may be assumed to be the same as that for the kinetic energy of dissipative eddies in turbulence; that is, $e_d \sim (\varepsilon\lambda)^{2/3}$, where ε is the rate of energy dissipation in water and λ is the Kolmogorov microscale, which characterizes the dissipative eddies in turbulence (Landau and Lifshitz, 1993). The order of magnitude for the rate of energy dissipation in turbulent flow is $\varepsilon \sim (\Delta u)^3/l$, where Δu is the velocity fluctuation with respect to the mean velocity u, and l is the Kolmogorov macroscale, which is the minimum dimension of the turbulent flow field (Landau and Lifshitz, 1993; Tennekes and Lumley, 1972). For the turbulent flow in the static mixer, the magnitudes for λ and l may be taken, respectively, as the drop diameter and the inner diameter of the mixer. An analysis of scale relations in turbulence suggests that $\Delta u/u \sim \lambda/l$; thus, $\varepsilon\lambda \sim (\lambda/l)^4u^3 = (D/D_0)^4u^3$. Therefore, $E_d/E_s \sim (D/D_0)^{11/3}(u^2\rho D_0/\sigma) = (D/D_0)^{11/3}$, where $\mathrm{We} = u^2\rho D_0/\sigma$ is the Weber number. The scale ratio $D/D_0 = \lambda/l$ is inversely proportional to the Reynolds number (Tennekes and Lumley, 1972). Because the sizes of the stable drops are associated with the Weber number, the Weber number may better characterize the scale ratio for a disperse-drop flow. Thus, it is reasonable to assume that $(D/D_0)^{11/3} \sim \mathrm{We}^{-m}$, where the power m depends on the intensity of turbulence. Then the disruptive-to-surface energy ratio may be given as

$$E_d/E_s = \alpha\ \mathrm{We}^n \tag{6}$$

where α is a constant and the power n ($=1 - m$) needs to be determined experimentally. Because Eq. 6 is a result of an order-of-magnitude analysis, Eq. 5 may be expressed in a simple form as

$$SMD/D_0 = C\ \mathrm{We}^n \tag{7}$$

where C is a constant. Note that Eq. 7 holds only for a fully developed turbulent flow. Figure 8 shows the dependency of the nondimensionalized Sauter mean diameter on the Weber number for eight sets of experimental data for disperse CO_2-drop flows in the static mixer. Under the experimental conditions, the $SMD/D_0 = f(\mathrm{We})$ relationship is found to be

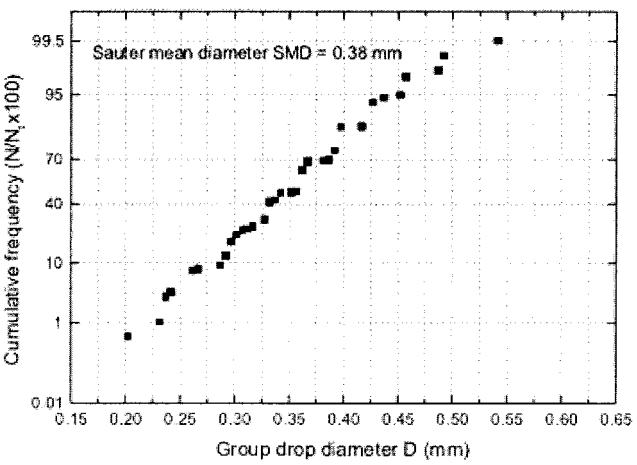

Figure 7. Cumulative frequency of the CO_2 drop diameter observed for case (b) in Figure 4.

Conditions: pressure = 7.0 MPa; temperature = 278 K; CO_2 flow rate = 46.6 mL/min; water flow rate = 2,063 mL/min.

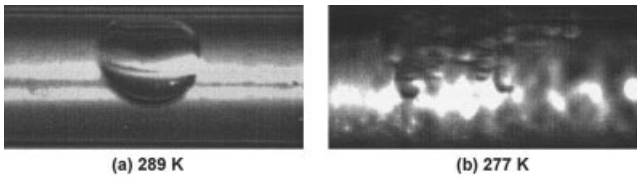

Figure 9. Slug and sluglike flows of liquid CO_2 drops observed under a laminar flow condition of water (Re = 964).

(a) Slug flow out of the hydrate formation condition (pressure = 7.0 MPa, temperature = 289 K); (b) sluglike flow under the hydrate formation condition (pressure = 7.0 MPa, temperature = 277 K).

$$SMD/D_0 = 0.29\ \mathrm{We}^{-0.48} \tag{8}$$

that is, $C = 0.29$ and $n = -0.48$. It is seen in Figure 8 that the relationship between SMD/D_0 and We is well characterized by Eq. 8. Equation 8 indicates that, for the disperse CO_2-drop flow in the static mixer, the average drop size can be reasonably predicted on the basis of given pressure and temperature of the mixture and given conditions for the mixer and the flow. Therefore, the sizes of CO_2 drops released from the static mixer could be manageable.

Influence of dispersed-phase flow on drop sizes

Equation 8 holds only for a fully developed turbulent flow, under which the liquid CO_2 becomes fully dispersed and the disperse CO_2 drops have passive behavior because their motion is governed by the water flow. In this case, although coalescence of drops also takes place, drop breakup prevails in the disperse-drop flow; and, because the stable drops are small, their buoyancy becomes negligible compared to the hydrodynamic force to which they are subjected. However, if the corresponding water flow is laminar, then coalescence of the CO_2 drops before hydrate covers their surfaces and/or agglomeration of the CO_2 drops with a hydrate layer may become a competing process to that of the drop breakup. Thus, relatively large, irregular drops could be formed. For these large nonuniform drops, the order of magnitude of the buoyant force may reach that of the hydrodynamic force. When no longer subject to the agitation from the mixing elements, these drops may immediately form clusters as a combined result of drop buoyancy and coalescence/agglomeration. Then the corresponding two-phase flow pattern becomes a sluglike flow. If the temperature of the mixture is out of the hydrate formation region, then the two-phase flow becomes a regular slug flow, as shown in Figure 9.

Under a given laminar flow for water, increasing the CO_2 flow reduces the degree of coalescence/agglomeration. This is because the drop momentum in the flow direction increases and the drop residence time in the mixer decreases with increase in the CO_2 flow, both of which reduce the tendency for coalescence/agglomeration. In comparison, in a turbulent water flow, increasing the CO_2 flow increases the drop number density but it may not turn the passive behavior of the CO_2 drops into active; therefore, it insignificantly influences the sizes of the drops and their distribution. Figure 10 compares the effects of the CO_2 flow on the two-phase flow pattern under a laminar water flow with the Reynolds number Re = 964 and a turbulent water flow with Re = 4064. Figure 11 compares the mean drop diameter for the same water-flow conditions.

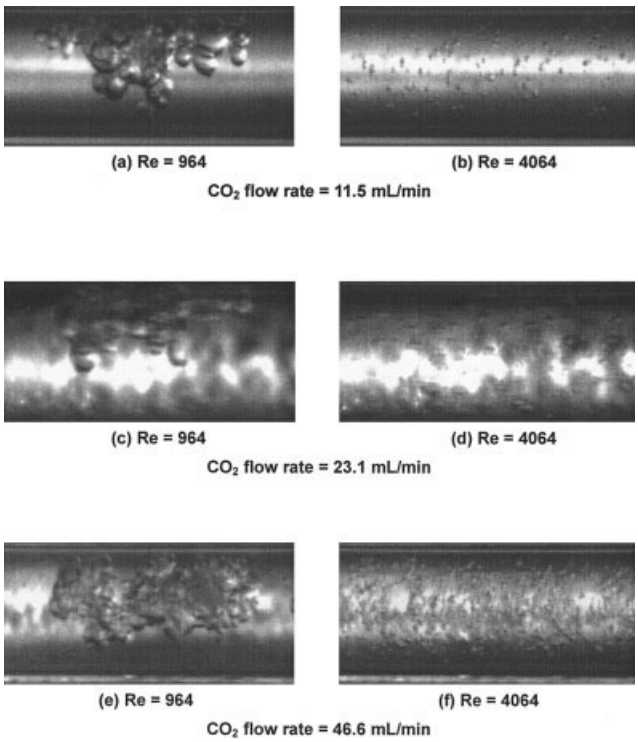

Figure 10. Two-phase flow patterns for various CO_2 flow conditions under a laminar flow condition (Re = 964, lower left) and a turbulent flow condition (Re = 4064, lower right) of water.

Pressure = 7.0 MPa, and temperature = 277 K.

It is seen in Figures 10 and 11 that the CO_2 flow affects the drop sizes and their distribution only at low water flows, under which the disperse CO_2-drop flow cannot be obtained and the discharge from the static mixer may be CO_2-drop clusters. Although the phenomena occurred in the downstream observation section, they may or may not be the same as in a direct release from the mixer; this possible release pattern should be

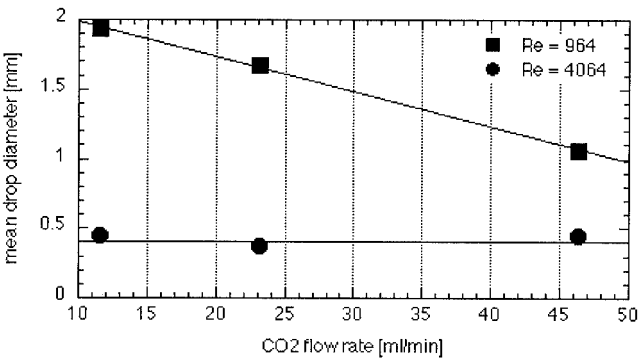

Figure 11. Effect of the CO_2 flow rate on the mean drop diameter under laminar water flow (Re = 964) and turbulent water flow (Re = 4064) conditions.

Pressure = 7.0 MPa, and temperature = 277 K.

avoided because of the following reasons: (1) the clusters may not be stable under the ocean turbulence and thus it is difficult to predict their dissolution; (2) the CO_2 concentration from such a release is much higher than that of the disperse CO_2-drop flow; and (3) if the mixing elements could not break these clusters in case they formed in the mixer, then the clusters may cause a blockage in the mixer. Thus, a turbulent flow in the static mixer is suggested.

Effect of hydrate formation on behavior of CO_2 drops in the static mixer

For all the cases in this study, no hydrate plugging occurred, although the rapid formation of hydrate layer at the interface of liquid CO_2 and water phase was observed under the thermodynamic conditions of hydrate formation ($p > 44.5$ bar, $T < 283$ K). An apparent difference between drops with and without a hydrate layer could be noticed in a not fully dispersed flow when the drops interacted with each other: those with hydrate tended to maintain their interfaces and form a cluster of drops and those without hydrate tended to coalesce into a larger drop or a liquid plug. In the disperse-drop flow cases, the drops with a hydrate layer were smaller in size and distributed more evenly than those without a hydrate layer under the same mixing and flow conditions.

Energy consumption associated with the mixture flow through the static mixer

Energy consumed in the static mixer for mixing is primarily provided by the kinetic energy of the CO_2 efflux and water. Energy consumption associated with the mixer may be analyzed in the following. The driving force for the CO_2–water (or seawater) mixture to flow through the static mixer is equal to the drop in pressure across the mixer, which may be determined from a force balance over the mixer as

$$\frac{\pi}{4} D_0^2 \Delta p = (\pi D_0 L + 2 D_0 L_0 n_E)\tau_W \tag{9}$$

where Δp is pressure drop over the mixer, and D_0 and L are, respectively, the inner diameter and length of the mixer; L_0 is the length of the mixing element, $n_E = L/L_0$ is the number of mixing elements (assuming a full arrangement of the mixing elements in the static mixer), and τ_W is the shear stress on the wall. Rearranging Eq. 9 leads to

$$\Delta p = 4 \frac{L}{D_0} (1 + 2/\pi)\tau_W \tag{10}$$

The shear stress τ_W may be expressed in the kinetic energy of the mixture flow as

$$\tau_W = f(\rho u^2/2) \tag{11}$$

where f is the Fanning coefficient, and ρ and u are the density and average velocity for the mixture, respectively. Combining Eqs. 10 and 11 yields

$$\Delta p = 4f(1 + 2/\pi) \frac{L}{D_0} \frac{\rho u^2}{2} \tag{12}$$

Because of the alternate rotation of the mixing elements, an extra local pressure drop is generated by each of the mixing elements, which may be described in the local pressure loss as

$$\Delta p_E = n_E K \frac{\rho u^2}{2} = K \frac{L}{L_0} \frac{\rho u^2}{2} \tag{13}$$

where K is the local pressure loss factor. Combining Eq. 13 into Eq. 12 yields

$$\Delta p = 4 f_{SM} \frac{L}{D_0} \frac{\rho u^2}{2} \tag{14}$$

with

$$f_{SM} = (1 + 2/\pi) f + \frac{K}{4} \frac{D_0}{L_0} = (1 + 2/\pi) f + K/6 \tag{15}$$

where f_{SM} is the effective Fanning coefficient for the static mixer and $L_0/D_0 = 1.5$ has been applied. Because both values for f and K vary with the Reynolds number, f_{SM} also is a function of the Reynolds number. Because for a disperse-drop flow the volume fraction of liquid CO_2 is too small to affect the total flow, the resistance and the energy dissipation in the mixture are characterized largely by the continuous phase (Berkman and Calabrese, 1988; Middleman, 1974). Therefore, Δp may be determined on the basis of water properties, implying that ρ, u, and the Reynolds number may be approximated by water properties. For the static mixer used in the experiment, the effective Fanning coefficient for the static mixer can be given as (Noritake Ltd. Co., 2000)

$$f_{SM} = f(K_{OL} + K'_{OL}\mathrm{Re}^{0.921}) \quad \text{for } 10 < \mathrm{Re} \le 2 \times 10^3 \tag{16a}$$

$$f_{SM} = f K_{OT} \mathrm{Re}^{0.1} \quad \text{for } 2 \times 10^3 < \mathrm{Re} < 10^5 \tag{16b}$$

where Re is the Reynolds number; K_{OL}, K'_{OL}, and K_{OT} are local pressure-loss factors, whose values could vary with changes in dimensions of the mixing elements.

The rate of energy dissipation in the unit mass of the mixture may be approximated as

$$\varepsilon = (\Delta p/\rho)/t_R \approx (\Delta p u)/(\rho L) \tag{17}$$

where $t_R \approx L/u$ is the residence time for the mixture in the mixer. Substituting Eq. 14 into Eq. 17 yields

$$\varepsilon = 2 f_{SM} u^3 / D_0 \tag{18}$$

As a case study, consider case (b) of Figure 4, which is a typical disperse-drop flow in the experiment. For this case, $p =$ 7.0 MPa and $T = 278$ K; water flow = 2,063 mL/min and liquid CO_2 flow = 46.6 mL/min; the mass fraction of CO_2 in the mixture is 0.02. Under the given conditions, corresponding

pressure drop and energy-dissipation rate are, respectively, $\Delta p = 6.9$ kPa and $\varepsilon = 4.6$ W/kg mixture. The energy-dissipation rate may be expressed alternatively in unit mass of CO_2 as 0.76 kW/kg CO_2. The residence time for the CO_2 in the static mixer is estimated to be 0.45 s; on the basis of the residence time and the energy-dissipation rate, an equivalent energy consumption is obtained as 0.34 kJ/kg CO_2 or 0.34 MJ/ton CO_2. This energy consumption is negligible compared to that for transportation of liquid CO_2 from the ocean surface to the disposal site.

Conclusions

A new method for releasing liquid CO_2 into the ocean at intermediate depths by a submerged Kenics-type static mixer was proposed and was validated at a laboratory-scale simulation. Features of this new method are summarized in the following:

- Because the release is a CO_2–seawater mixture where CO_2 drops become fully dispersed, the apparent CO_2 concentration of the release can be determined by the mixing rate, which can be justified according to the ambient condition.
- The dispersed CO_2 drops in the release are fairly uniform in size, which eases the prediction of the dissolution of the CO_2 drops released into the ocean.
- The Sauter mean diameter well represents the average size of the dispersed drops and the drop size distribution in the release obeys the normal distribution with respect to the Sauter mean diameter.
- The average size of the dispersed drops in the release correlates well with the Weber number on the basis of the continuous phase. This suggests that the average drop size in the release can be controlled by adjusting the rate of the seawater flowing through the mixer.

However, it needs to be pointed out that the field-scale phenomena may not be revealed fully in a laboratory-scale simulation because of the limited experimental conditions; thus, further studies should be conducted before this concept is applied in a field application.

Acknowledgments

The authors thank Shin-ichiro Ito (Noritake Ltd. Co.) for help and comments on the static mixer used in the experiment, and Professor Hakuai Inoue (Soka University, Japan) for fruitful discussions.

Literature Cited

Aya, I., K. Yamane, and N. Yamada, "Stability of Clathrate-Hydrate of Carbon Dioxide in Highly Pressured Water," *ASME-HTD*, **125**, 17 (1992).

Aya, I., K. Yamane, and N. Yamada, "Effect of CO_2 Concentration in Water on the Dissolution Rate of Its Clathrate," *Proceedings of the International Symposium on CO_2 Fixation and Efficient Utilization of Energy*, Tokyo, pp. 351–360 (1993).

Berkman, P. D., and R. V. Calabrese, "The Dispersion of Viscous Liquids by Turbulent Flow in a Static Mixer," *AIChE J.*, **34**, 602 (1988).

Brewer, P. G., G. E. Friederich, E. T. Peltzer, and F. M. Orr, Jr., "Direct Experiments on the Ocean Disposal of Fossil Fuel CO_2," *Science* **284**, 943 (1999).

Fujioka, Y., K. Takeuchi, Y. Shindo, and H. Komiyama, "Shrinkage of Liquid CO_2 Droplets in Water," *Int. J. Energy Res.*, **18**, 765 (1994).

Halmann, M. M., and M. Steinberg, *Greenhouse Gas Carbon Dioxide Mitigation: Science and Technology*, Lewis Publishers, Boca Raton, FL (1999).

Handa, N., and T. Ohsumi, eds., *Direct Ocean Disposal of Carbon Dioxide*, Terra Scientific Publishing Co., Tokyo, Japan (1995).

Haugan, P. M., and H. Drange, "Sequestration of CO_2 in the Deep Ocean by Shallow Injection," *Nature*, **357**, 318 (1992).

Herzog, H. J., E. M. Drake, and E. E. Adams, "CO_2 Capture, Reuse and Storage Technologies for Mitigating Global Climate Change—A White Paper," DOE Order No. E-AF22–96PC01257 (1997), http://sequestration.mit.edu/pdf/WhitePaper.pdf

Kojima T., and B. Harrison, *The Carbon Dioxide Problem: Integrated Energy and Environmental Policies for the 21st Century*, Gordon & Breach Science Publishers, Australia (1998).

Landau, L. D., and E. M. Lifshitz, *Course of Theoretical Physics: Fluid Mechanics,* Vol. 6, 2nd ed., Pergamon Press, Oxford, UK (1993).

Liro, C. R., E. E. Adams, and H. J. Herzog, "Modeling the Release of CO_2 in the Deep Ocean," *Energy Convers. Mgmt*., **33**, 667 (1992).

Middleman, S., "Drop Size Distributions Produced by Turbulent Pipe Flow of Immiscible Fluids through a Static Mixer," *Ind. Eng. Chem. Process Des. & Dev*., **13**, 78 (1974).

Nakashiki, N., T. Ohsumi, and Y. Shitashima, "Sequestering of CO_2 in a Deep Ocean Fall Velocity and Dissolution Rate of Solid CO_2 in the Ocean," CRIEPI report (EU91003), Japan (1991).

Noritake Co., Ltd., *The Basic Technology of Static Mixers* (in Japanese), Technical Report No. 26, Noritake Co., Nagoya, Japan (2000).

Ogasawara, K., A. Yamasaki, and H. Teng, "Mass Transfer from CO_2 Drops Traveling in High-Pressure and Low-Temperature Water," *Energy & Fuels*, **15**, 147 (2000).

Ozaki, M., "CO_2 Injection and Dispersion in Mid-Ocean by Moving Ship," *Waste Management*, **17**, 369 (1997).

Saito, T., T. Kajishima, and R. Nagaosa, "CO_2 Sequestration at Sea by Gas-Lift System of Shallow Injection and Deep Releasing," *Environ. Sci. Technol.,* **34**, 4140 (2000).

Saji, A., H. Yoshida, M. Sakai, T. Tanii, T. Kamata, and H. Kitamura, "Fixation of Carbon Dioxide by Clathrate-Hydrate," *Energy Convers. Mgmt.*, **33**, 643 (1992).

Sakai, H., T. Gamo, E. S. Kim, M. Trutsumi, T. Tanaka, J. Ishibashi, H. Wakita, M. Yamamoto, and T. Oomori, "Venting of Carbon Dioxide-Rich Fluid and Hydrate Formation in the Mid-Okinawa Trough Backarc Basin," *Science*, **248**, 1093 (1990).

Sato, T., and T. Hama, "Numerical Simulation of Dilution Process in CO_2 Ocean Sequestration," *Proceedings of the 5th International Conference on Greenhouse Gas Control Technologies*, CSIRO, Colingwood, Australia, pp. 475–480 (2001).

Sloan, E., *Clathrate Hydrate of Natural Gases*, 2nd ed., Marcel Dekker, New York (1998).

Song, K. Y., and R. Kobayashi, "Water Content of CO_2 in Equilibrium with Liquid Water and/or Hydrates," *SPE Formation Evaluation*, **December**, 500 (1987).

Steinberg, M., *A System Study for the Removal, Recovery, and Disposal of Carbon Dioxide from Fossil Fuel Power Plant in the U.S.*, USDOE Report, US-DOE/CH/00016-2, U.S. Dept. of Energy, Washington, DC (1984).

Teng, H., A. Yamasaki, and Y. Shindo, "Effect of Hydrates on Instability of Liquid CO_2 Jet in the Deep Ocean," *Energy*, **22**, 273 (1997).

Tennekes, H., and J. L. Lumley, *A First Course in Turbulence*, The MIT Press, Cambridge, MA (1972).

Yamasaki, A., M. Wakatsuki, H. Teng, Y. Yanagisawa, and K. Yamada, "A New Ocean Disposal Scenario for Anthropogenic CO_2: CO_2 Hydrate Formation in a Submerged Crystallizer and Its Disposal," *Energy*, **25**, 85 (2000).

Manuscript received Jan. 7, 2003, revision received Aug. 6, 2003, and final revision received Dec. 18, 2003.